VI CONGRESSO NACIONAL DE ENGENHARIA MECÂNICA
VI NATIONAL CONGRESS OF MECHANICAL ENGINEERING
18 a 21 de agosto de 2010 – Campina Grande – Paraíba - Brasil
August 18 – 21, 2010 – Campina Grande – Paraíba – Brazil

EXPERIMENTAL AND NUMERICAL INVESTIGATION OF A PIEZO-AERO-ELASTIC WING

Wander Gustavo Rocha Vieira, wandergrv@gmail.com [1]
Carlos De Marqui Junior, demarqui@sc.usp.br[1]
Saulo Francelino Tristão, tristao.saulo@gmail.com[1]
[1]Universidade de São Paulo, Escola de Engenharia de São Carlos, Departamento de Engenharia de Materiais, Aeronáutica e Automobilística, Av. Trabalhador Sancarlense, 400. Cep 13566-590, São Carlos, São Paulo

Resumo:
Multifunctional structures can perform tasks additional to their primary functions and are pointed out as a future breakthrough technology for Unmanned Air Vehicles (UAV) design. Based on the concept of vibration-based energy harvesting, the lifting surfaces of a UAV can perform the additional function of providing electrical energy by converting aeroelastic vibrations to electricity using the direct piezoelectric effect. In this paper, the experimental and numerical investigation of a piezo-aero-elastic cantilevered plate-like wing with embedded piezoceramics are presented for energy harvesting. The piezo-aero-elastic model is obtained by combining na electromechanically coupled finite element model and an unsteady aerodynamic model. The electromechanically coupled finite element model is based on Kirchhoff assumptions to model the thin cantilevered wing with embedded piezoceramics layers. The substructure and the piezoceramic layers are assumed to be perfectly bonded to each other. A resistive load is considered in the electrical domain and the purpose is to estimate the power generated in the electrical domain due to the aeroelastic vibrations of the energy harvester wing. The aerodynamic model is accomplished with an unsteady doublet lattice model. The electromechanical and the aerodynamic models are combined to obtain the piezo-aero-elastic equations which are solved using a modified P-K scheme. The experimental wing is a spring steel plate of constant thickness and the aerodynamic shape is given by 12 pieces of NACA 0012 airfoil plates made of foam. Two layers of piezoceramics are bonded into the top and on the bottom of the plate. Wind tunnel tests are performed and the evolution of damping and frequencies of each aeroelastic mode as well as the electrical outputs (voltage, current and electrical power) are obtained for different airflow speeds and a given load resistance. The experimental data is used to verify the piezo-aero-elastic model predictions.

Palavras-chave: *Aeroelasticity; Piezo-aero-elastic; Flutter; Doublet-lattice; Piezoceramics*

1. INTRODUÇÃO

Multifunctional structures are pointed out as a future breakthrough technology for the design of Micro Air Vehicles (MAVs) and Unmanned Air Vehicles (UAVs). A possible additional task to the primary load carrying function of aircraft structures is to provide an additional source of electrical energy by converting vibrations available in their environment to electricity through the concept of vibration-based energy harvesting. UAVs and MAVs constitute unique application systems where the possibility of an additional and localized energy source is very important. An additional energy source to run small electronic devices during the flight has the practical value of relieving auxiliary power sources of unmanned aircraft. A possible source of low-level energy for UAVs and MAVs is the mechanical vibration energy due to unsteady aerodynamic loads during the flight or due to ground excitation in perching. Although other transduction mechanisms exist, piezoelectric transduction has received the most attention for vibration-based energy harvesting (Sodano et al, 2004) due to large power density it provides. Piezoelectric power generators can harvest electrical energy from mechanical vibrations based on the direct piezoelectric effect. Researchers have proposed various models to represent the electromechanical behavior of piezoelectric energy harvesters over the last five years (Erturk and Inman, 2009a). More recently, the analytical distributed parameter solutions for unimorph and bimorph piezoelectric energy harvester configurations with closed-form expressions have been presented (Erturk and Inman, 2008;Erturk, and Inman, 2009b). An electromechanically coupled finite element (FE) formulation is another way of modeling the dynamics of piezoelectric energy harvesters. Recently an electromechanically coupled FE model (De Marqui Junior et al, 2009a) has been successfully verified against the analytical results obtained from the closed-form solution for a unimorph harvester under base excitation (Erturk and Inman, 2008) and also against the analytical and experimental results for a bimorph harvester with a tip mass under base excitation (Erturk and Inman, 2009c). The FE model has also been used to solve an optimization problem for UAV applications. The aluminum wing spar of a UAV is modified to design a generator wing spar. Since mass densities of typical piezoceramics are considerably large for UAV

applications, a limiting value for mass addition is imposed to the problem as a design constraint. Dimensions of the embedded piezoceramic are identified for the maximum electrical power output of the generator spar with embedded piezoceramics.

The piezoaeroelastic modeling of the concept of a piezoelectric generator wing with embedded piezoceramics (two identical layers, on the top and bottom surfaces, with the same width of the wing chord and covering 30% of the wing span, from the root to the tip) has also been presented (De Marqui Junior et al, 2009b) . The coupled model is obtained from the combination of the electromechanically coupled FE model (De Marqui Junior et al, 2009a) with an unsteady vortex lattice model. In solving the piezoaeroelastic equations of motion in time domain, a particular issue is addressed: the dependence between aerodynamic and electromechanical domains, i.e., to obtain the aerodynamic loads one must know the structural motion whereas to know the structural motion it is necessary to know the aerodynamic loads. The conversion of aeroelastic vibrations into electrical energy is investigated at several airflow speeds for a set of electrical load resistances. The aeroelastic behavior, and consequently the power generation, is dependent on aerodynamic damping which is modified with increasing airflow speed. At the flutter speed, the aerodynamic damping vanishes and the oscillations are persistent. Although this condition is avoided in a real aircraft, this is the best condition as a concept demonstration for the generator wing investigated here using the linear piezoaeroelastic model. The response history with the largest power output at the flutter speed shows a decaying behavior which is due to the shunt damping effect of power generation. The effect of segmented electrodes on the piezoaeroelastic response of the same generator wing and same set of load resistances has also been investigated (De Marqui Junior et al, 2009c). The electrodes are segmented on the center line (mid-chord position) and properly combined to the electrical load to avoid the cancelation of the potential electrical output of the torsion-dominated modes (which is strongly cancelled when continuous electrodes are used).

As a consequence of the improved electromechanical coupling better power generation and shunt damping effects are obtained for the aeroelastic behavior since the piezoelectric reaction of the torsional modes in the coupled aeroelastic motions of flutter are taken into account with the segmented-electrode configuration.

In this paper, frequency domain piezoaeroelastic analysis of a generator wing with two pairs of piezoceramics is presented for energy harvesting. The electromechanical finite element plate model is based on the Kirchhoff assumptions. A resistive load is considered in the external circuit. The subsonic unsteady aerodynamic model is accomplished with the doublet lattice method. The electromechanical and the aerodynamic models are combined to obtain the piezoaeroelastic equations, which are solved using a modified p-k scheme that accounts the electromechanical coupling. The evolution of the aerodynamic damping and frequencies is presented for each mode with increasing airflow speed under fixed load resistance. Usually, conductive electrode pairs cover the surfaces of the piezoceramic layers continuously. The electrical charge collected by the electrodes covering the surfaces of the piezoceramic layers is a function of the electric displacement in the piezoceramic during vibrations and the electric displacement is function of the dynamic strain distribution throughout the area of the wing. Therefore cancelation of electrical output occurs for modes of a cantilevered wing other than the fundamental bending mode when continuous electrodes are used. A consequence of the use of segmented electrodes (or sets of piezoceramics) is the improved electromechanical coupling and power generation since the piezoelectric reaction of torsional modes are taken into account at flutter. Two different combinations for the piezoceramics on the surface of the generator wing are used and the piezoaeroelastic evolution with increasing airflow speed is investigated. Piezoaeroelastic wind tunnel verifications are also presented in this paper.

2. PIEZOAEROELASTIC MODEL

The piezoaeroelastic model is obtained by combining an electromechanically coupled FE model and an unsteady doublet-lattice aerodynamic model. The electromechanically coupled FE model is based on the Kirchhoff assumptions to model the thin cantilevered wing with embedded piezoceramic layers shown in Fig. 1.

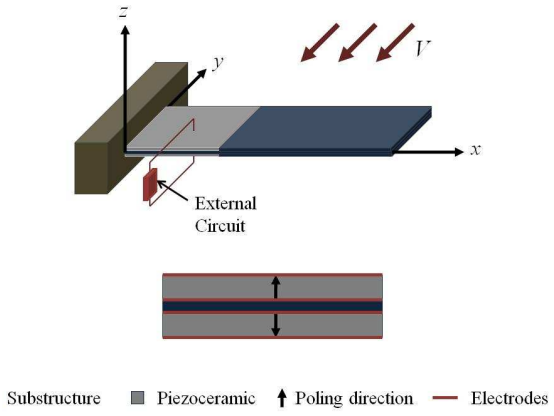

Figure 1 - Thin cantilevered wing with embedded piezoceramic layers and its cross-section.

The substructure and the piezoceramic layers are assumed to be perfectly bonded to each other. The piezoceramic layers (which are poled in the thickness direction) are covered by continuous electrodes (which are assumed to be perfectly conductive) with negligible thickness. A resistive load and a resistive-inductive circuit will be considered in the electrical domain. The purpose is to estimate the power generated in the electrical domain due to the aeroelastic vibrations of the energy harvester wing as well as the influence over electrical power generation on the aeroelastic behavior of the wing. A rectangular finite element with four nodes and three mechanical degrees of freedom per node is used to model the substructure. An electrical degree of freedom is added to the finite element to model the piezoceramic layers (13 degrees of freedom in total). A transformation is imposed in order to account for the presence of continuous and conductive electrodes bracketing each piezoceramic layer. This way a single electrical output is obtained from each piezoceramic layer. The reader is referred to De Marqui Junior et al.(2009a) for the detailed derivation and validation of the electromechanically coupled FE model against the analytical and the experimental results.

The governing piezoaeroelastic equations for the generator wing (Fig. 1) are Eq. 1 and Eq. 2.

$$\mathbf{M}\ddot{\boldsymbol{\Psi}} + \mathbf{C}\dot{\boldsymbol{\Psi}} + \mathbf{K}\boldsymbol{\Psi} - \tilde{\boldsymbol{\Theta}} v_p = \mathbf{F} \tag{1}$$

$$\bar{C}_p \dot{v}_p + v_p Y + \tilde{\boldsymbol{\Theta}}^t \dot{\boldsymbol{\Psi}} = 0 \tag{2}$$

where **M** is the global mass matrix, **K** is the global stiffness matrix, **C** is the global damping matrix (assumed here as proportional to the mass and the stiffness matrices), $\tilde{\boldsymbol{\Theta}}$ is the effective electromechanical coupling vector, C_p is the effective capacitance of the piezoceramic, and Y is the admittance of the external circuit. It is known from the literature (Erturk et al, 2009c; Wang and Cross, 1999) that the electrode pairs covering each piezoceramic layer of a bimorph (Fig. 1) can be connected in series or in parallel to the external electrical load (for larger voltage or current). In general, the piezoceramic layers are poled in the same direction for parallel connection whereas they are poled in the opposite direction for series connection. For the parallel connection case, the effective electromechanical coupling vector is the sum of the individual contribution of each layer and the effective capacitance is the sum of each individual capacitances. For the series connection case, the effective electromechanical coupling vector is equal to that of one piezoceramic layer and the effective capacitance is one half of the capacitance of one piezoceramic layer. In the case studies presented here, the continuous electrodes covering the piezoceramic layers (poled in the opposite directions) are connected in series to an external circuit (cross-section in Fig. 1). The right-hand-side of the mechanical equation (Eq.1) is the vector of unsteady aerodynamic loads obtained from the unsteady doublet-lattice solution.

2.1. Unsteady Aerodynamic Model

The Doublet-Lattice Method (DLM) is a well-known and usual method to determine the unsteady aerodynamics loads in aeroelastic problems. The DLM is a linearized formulation for the oscillatory, inviscid, subsonic lifting surface theory that relates the normal velocity at the surface of a body (e.g. an elastic wing) with the aerodynamic loads caused by the pressure distribution (E. Albano et al, 1970). The formulation was presented by Albano and Rodden (1970), and since then several authors (Blair, M, 1992; J.P. Giesing, et al, 1971; Rodden, W.P.,1994), has used the DLM for flutter investigations.

The formulation of DLM is derived using the unsteady Euler equations of the surrounding fluid. The assumption of small perturbations about a uniform stream is assumed in order to linearize the set of equations. The velocity field behavior is described by the aerodynamic potential equation (Eq.3).

$$\left(1-M^2\right)\phi_{xx} + \phi_{yy} + \phi_{zz} - \left(\frac{2V}{a^2}\right)\phi_{xt} - \left(\frac{1}{a^2}\right)\phi_{tt} = 0 \tag{3}$$

Where *M* is the Mach number, *V* is the air flow velocity, ϕ is the potential variable, a is the speed of sound. The subscripts indicate differentiation with respect to the space and time variables.

Three boundary conditions are defined for the problem: (1) on the trailing edge wake by inexistence of doublet along the wing plane, (2) the uniform flow is assumed at the far field (automatically satisfied by doublet singularities), (3) the normal velocity on the wing surface is given by the structural motion in presence of unsteady aerodynamic loads. By this, there is the Equation 4.

$$w = \frac{\partial h}{\partial h} + V\frac{\partial h}{\partial x} \tag{4}$$

Where, $w = \phi_z$ and h is the normal position of medium plane of the wing.

It is also necessary to describe the resultant differential pressure across the surface of a wing given the boundary condition of transverse velocity field (Blair, M , 1992).

$$\left(1-M^2\right)p_{xx}+p_{yy}+p_{zz}-\left(\frac{2V}{a^2}\right)p_{xt}-\left(\frac{1}{a^2}\right)p_{tt}=0 \tag{5}$$

In Equation 5 p is the pressure.

The relation between the aerodynamic potential and the pressure potential is found through the unsteady linearized Bernoulli equation (Eq.6).

$$p=\phi_t+V\phi_x \tag{6}$$

Using the analogy with the acoustic potential one can observe that the doublet singularity is a solution for aerodynamic potential equation. Similarly, the equivalent pressure doublet is an elementary solution for pressure equation. After some mathematical steps, the relation between the normal velocity along the wing and the pressure difference across the surface of wing is obtained as Equation 7.

$$\bar{w}\left(x,y,z\right)=\frac{-1}{4V\pi\rho_o}\iint_S\Delta p\left(x,y,z\right)K\left(x-\xi,y-\eta,z\right)d\xi d\eta \tag{7}$$

Where $\Delta p\left(x,y,z\right)$ is the differential pressure, V is the free-stream velocity, ρ_o is the air density, ξ and η are dummy variables of integration over the area S of the wing in x (chord-wise) and y (span-wise) direction, z is the transverse direction and K is the kernel function. The kernel function is a closed-form solution of the integro-differential equation based on the assumption of harmonic motion and it is given by

$$K\left(x-\xi,y-\eta,z\right)=\exp\left(\frac{-j\omega\left(x-\xi\right)}{V}\right)\frac{\partial^2}{\partial z^2}\left[\frac{1}{\bar{R}}\exp\left[\frac{j\omega}{V\beta^2}\left(\lambda-M\bar{R}\right)\right]d\lambda\right] \tag{8}$$

where $\beta^2=1-M^2$ and $\bar{R}=\sqrt{\left(x-\xi\right)^2+\left(y-\eta\right)^2+z^2}$, ω is the frequency of excitation, M is the Mach number and λ is a dummy variable.

The DLM provides a numerical approximation for the solution of the kernel function. The wing is represented by a thin lifting surface divided into a number of elements (panels or boxes) with doublet singularities of constant strength in chord-wise and parabolic strength in span-wise direction. A line of doublets (distribution of acceleration potential) is assumed at the ¼ chord line of each panel, which is equivalent to a pressure jump across the surface. A control point is defined in the half span of each box at the ¾ chord line (the point where the boundary condition is verified). The strength of the oscillating potential placed the ¼ chord lines are the unknowns of the problem.

The prescribed downwash (as the solution is assumed to be harmonic) introduced by the lifting lines is checked at each control point. The solution of the resulting matrix equation is

$$\frac{\bar{\mathbf{w}}}{V}=\mathbf{A}\left(M,k\right)\Delta\mathbf{C}_p \tag{9}$$

which gives the strength of the lifting line at each panel and consequently the pressure distribution across the surface. Here, $\mathbf{A}$ is the matrix of influence (which is related to the kernel function) between the normal velocity and the non-dimensional pressure distribution $\Delta\mathbf{C}_p$ and $k=\omega b/V$ is the reduced frequency, b is the semichord. Integration over the area gives the local and consequently the total aerodynamic force coefficients.

2.2. Piezoaeroelastically Coupled Equations of Motion

The aerodynamic loads can be included in the piezoaeroelastic equations as an aerodynamic matrix of influence coefficients. The aerodynamic loads and the structural motion are obtained from distinct numerical methods with distinct meshes. Therefore transformation matrices are determined using a surface infinite plate spline scheme in order to interpolate the forces obtained in the DLM mesh to the nodes of the FE mesh. The resulting transverse displacements and rotation in the chord direction at the structural mesh are also interpolated to the control points of the aerodynamic mesh.

The aerodynamic force can be written in the modal domain. The boundary condition is added on the downwash by the input of structural mode shape obtained using the FE,

$$\mathbf{F_a} = q\mathbf{G_{sa}}\mathbf{S_{area}}\mathbf{A}^{-1}\left(\frac{1}{V}\frac{\partial(\mathbf{G_{as}}\mathbf{\Phi}_w)}{\partial t} + k\frac{\partial(\mathbf{G_{as}}\mathbf{\Phi}_w)}{\partial x}\right)\boldsymbol{\eta} \tag{10}$$

where q is the dynamic pressure, $\mathbf{G_{sa}}$ the transformation matrix (aerodynamic to structural mesh), $\mathbf{\Phi_w}$ is the modal matrix and $\boldsymbol{\eta}$ the modal coordinates. An influence aerodynamic matrix is created,

$$\mathbf{Q} = \mathbf{\Phi}^t\mathbf{G_{sa}}\mathbf{S_{area}}\mathbf{A}^{-1}\left(\frac{1}{V}\frac{\partial(\mathbf{G_{as}}\mathbf{\Phi_w})}{\partial t} + k\frac{\partial(\mathbf{G_{as}}\mathbf{\Phi_w})}{\partial x}\right) \tag{11}$$

Since the unsteady aerodynamic solution is assumed to be harmonic, the piezoaeroelastic equations ((Eq. 1) and Eq.2)) in modal domain can be presented as,

$$\left(-\omega^2\bar{\mathbf{M}} + j\omega\bar{\mathbf{C}} + \bar{\mathbf{K}} - q\mathbf{Q}\right)\boldsymbol{\eta} - \mathbf{\Phi}^t\tilde{\mathbf{\Theta}}v_p = 0 \tag{12}$$

$$C_p j\omega v_p + v_p Y(\omega) + j\omega\tilde{\mathbf{\Theta}}^t\mathbf{\Phi}\boldsymbol{\eta} = 0 \tag{13}$$

where the over-bars represent modal matrices, j is the unit imaginary number and ω the circular frequency. The admittance $Y(\omega)$ depends on the external circuit. The admittance expressions for the resistive and the resistive-inductive (in series and in parallel) circuits are presented in Table 1.

Table 1 – Admittances for different external circuits.

External circuit	**Resistive**	**Resistive-inductive (in series)**	**Resistive-inductive (in parallel)**
Admittance	$\frac{1}{R_l}$	$\frac{1}{R_l + j\omega L}$	$\frac{1}{R_l} + \frac{1}{j\omega L}$

The conventional p-k scheme is one of the available ways to address the flutter equations for unsteady aerodynamic theories with the harmonic motion assumption. In this method, the evolution of the frequencies and damping is iteratively investigated for different airflow speeds (or reduced frequencies) solving the following eigenvalue problem for a conventional wing,

$$p\begin{Bmatrix}\mathbf{h}_1\\ \mathbf{h}_2\end{Bmatrix} = \begin{bmatrix}\mathbf{0} & \mathbf{I}\\ -\bar{\mathbf{M}}^{-1}\left(\bar{\mathbf{K}} - q\mathbf{Q}^R\right) & -\bar{\mathbf{M}}^{-1}\left(\bar{\mathbf{C}} - q\mathbf{Q}^I\right)\end{bmatrix}\begin{Bmatrix}\mathbf{h}_1\\ \mathbf{h}_2\end{Bmatrix} \tag{14}$$

where $\mathbf{h}_1 = \boldsymbol{\eta}$ and $\mathbf{h}_2 = p\boldsymbol{\eta}$, the superscripts R and I stand for the real and the imaginary parts of the aerodynamic matrix, p is the eigenvalue of the problem which gives the frequency (related to the imaginary part) and damping (related to the real part). However, Eqs. (12) and (13) differ from the conventional flutter equation due to the presence of piezoelectric layers and an external generator circuit (electromechanical coupling in the mechanical equation and the electrical equation, Eqs. (5) and (6)). Therefore the conventional p-k scheme is modified to solve the piezoaeroelastic problem for different electrical boundary conditions. For the first case (a resistive load) an augmented system is solved to examine the piezoaeroelastic behavior with increasing airflow speed and one specific load resistance using

$$p\begin{Bmatrix}\mathbf{h}_1\\ \mathbf{h}_2\\ h_3\end{Bmatrix} = \begin{bmatrix}\mathbf{0} & \mathbf{I} & \mathbf{0}\\ -\bar{\mathbf{M}}^{-1}\left(\bar{\mathbf{K}} - q\mathbf{Q}^R\right) & -\bar{\mathbf{M}}^{-1}\left(\bar{\mathbf{C}} - q\mathbf{Q}^I\right) & -\bar{\mathbf{M}}^{-1}\left(\mathbf{\Phi}\tilde{\mathbf{\Theta}}\right)\\ \mathbf{0} & \frac{\tilde{\mathbf{\Theta}}\mathbf{\Phi}}{C_p} & -\frac{1}{C_p R_l}\end{bmatrix}\begin{Bmatrix}\mathbf{h}_1\\ \mathbf{h}_2\\ h_3\end{Bmatrix} \tag{15}$$

where $\mathbf{h}_1 = \boldsymbol{\eta}$ and $\mathbf{h}_2 = p\boldsymbol{\eta}$, and $h_3 = v_p$ (the voltage output). The modified solution still gives the evolution of frequency and damping of the modes with increasing airflow speed as in the conventional p-k solution, but here the electromechanical coupling and the effect of a load resistance connected to the piezoceramic layer are considered. Although the main motivation here is electrical power generation, this formulation can be used to investigate the influence of the electrical domain (a resistive, resistive-inductive, or a more complex circuit) on the aeroelastic behavior of a generator wing.

In addition the modified p-k scheme (which gives the neutral stability limit) the piezoaeroelastic behavior can be investigated in terms of piezoaeroelastically coupled FRFs. The FRFs are defined using the Eqs. (12) and (13) assuming an imposed base excitation condition in the piezoaeroelastic problem. Therefore, the forcing term in Eq. (1) is modified as

$$\mathbf{F} = \mathbf{F}_{\mathbf{aero}} + \mathbf{F}_{\mathbf{b}} \tag{16}$$

where F_{aero} is the unsteady aerodynamic loads determined using the doublet lattice method ($F_{aero} = qQ$) and F_b is related to the base excitation. As discussed in the literature[3], if the base is vibrating in the transverse direction (*z*-direction), the effective force on the structure is due to the inertia of the structure in the same direction. Therefore, the forcing term F_b is represented as

$$\mathbf{F}_{\mathbf{b}} = \mathbf{m}^* a_b \tag{17}$$

where m^* is the vector of effective mass per unit area obtained from the FE solution (including both the piezoceramic and/or the substructure layers) and a_b is the base acceleration. Assuming the harmonic motion of the cantilevered base of the generator wing (root) with the influence of the unsteady aerodynamics, the piezoaeroelastically coupled FRFs are defined by the matrix equation,

$$\mathbf{FRF}s = \begin{pmatrix} -\omega^2 \bar{\mathbf{M}} + j\omega\bar{\mathbf{B}} + \bar{\mathbf{K}} - q\bar{\mathbf{Q}} & -\tilde{\boldsymbol{\Theta}} \\ j\tilde{\boldsymbol{\Theta}}\omega & jC_p\omega + Y(\omega) \end{pmatrix} \mathbf{m}^* \tag{18}$$

where **FRF**s is a $(n+1)$x 1 vector containing the *n* modal displacements per base acceleration (*n* is the number of modes considered in the solution) for a desired airflow speed. The line $(n+1)$ gives the steady-state voltage FRF defined here as the voltage per base acceleration for a desired airflow speed. In addition to the voltage FRF, one might as well define the power FRF. Assuming a resistive or a resistive-inductive circuit in parallel connection one can obtain the electric current FRF by dividing the voltage FRF to the load resistance R_l of the energy harvesting circuit. The electrical power FRF is the product of voltage and current FRFs and it is defined as the ratio of electrical power output to the square of the base acceleration.

When a simple resistive load is assumed, the variation of power output with load resistance at the short-circuit resonance frequency of a specific mode at a desired airflow speed can be investigated with the formulation presented here. This way the optimum load resistance for the maximum power or the maximum shunt damping can be determined for a desired airflow speed and vibration mode of interest. The typical aeroelastic behavior at this speed of neutral stability results in continuous power generation, i.e. the modes is coupled at the flutter frequency and self-sustained oscillations are obtained (zero aerodynamic damping). The optimum load resistance can be determined at the flutter speed (or at airflow speeds slightly smaller than the flutter speed) exciting the generator wing at the short circuit flutter frequency and investigating the power output. The optimum load resistance for maximum resistive shunt damping effect can also be determined by exciting the generator wing at the short circuit flutter frequency and investigating the relative tip motion.

2.3. Theoretical Analysis

This section presents numerical analysis of the piezoaeroelastic behavior of a cantilevered plate-like wing with four identical piezoceramics (QP10N, Midé Technology Corporation), two of them on the top and two on the bottom of the plate (Fig. 2). The piezoceramic patches on the same side (A1 and A2) are assumed poled in the same direction and opposed to the pair (B1 and B2) on the other side.

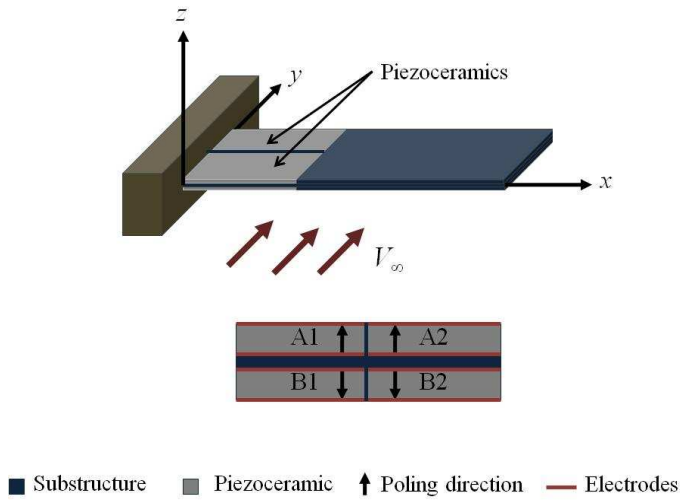

Figure 2. Power generator wing with piezoceramics (series connection).

The four quick packs on the wing can be connected in different ways to improve energy harvesting from bending or torsion modes. Although a bending mode gets unstable in the present investigation there are significant torsion motions in the coupled flutter condition. The alternative considered in the case study of this work is to combine the resulting electrical outputs of the upper (A1 and A2) and lower (B1 and B2) piezoceramics in series. Parallel connection of A1 and A2 (top of each one connected to one terminal of a load resistance) and parallel connection B1 and B2 (top of each one connected to one terminal of a load resistance). To avoid cancellation of the electrical output of the torsional mode the parallel connection of A1 and A2 can be combined with the parallel connection of B1 and B2 as follows: the bottom electrode of A1, the top electrode of A2, the top electrode of B1 and the bottom electrode of B2 are connected. The top electrode of A1 and the bottom electrode of A2 are connected to one terminal of the electrical load whereas the bottom electrode of B1 and the top electrode of B2 are connected to its opposite terminal. To avoid cancelation of the electrical output of bending modes the parallel connection of A1 and A2 can be combined with the parallel connection of B1 and B2 as follows: the bottom electrode of A1, the bottom electrode of A2, the top electrode of B1 and the top electrode of B2 are connected. The bottom electrode of A1 and the bottom electrode of A2 are connected to one terminal of the electrical load whereas the top electrode of B1 and the top electrode of B2 are connected to its opposite terminal. In the discussion given here, it is assumed that the substructure material does not provide conductivity between the electrodes. In practice, an epoxy or a Kapton layer is employed for this purpose. In practice and in the simulations presented here both connections discussed here do not change the aeroelastic stability of the wing.

The dimensions of the plate-like wing used in this work are 500 × 100 × 0.45 mm^3. The geometric and the material properties of the wing (spring steel) are presented in Table 2. Note that the length - to - thickness ratio of the wing is large enough to neglect the shear deformation and the rotary inertia effects for the vibration modes of interest. The typical properties of PZT-5A piezoceramics are given in Table 3.

Table 2. Geometric and material properties of the spring steel wing with piezoceramics

Length of the wing (mm)	500
Width of the wing (mm)	100
Thickness of the wing (mm)	0.45
Young's modulus of the wing (GPa)	207.0
Mass density of the substructure (kg/m^3)	7800
Proportional constant – α (rad/s)	0.1603
Proportional constant – β (s/rad)	4.3084 x 10^{-4}

Table 3. Material and electromechanical properties of PZT-5A

Mass density (kg/m^3)	7800
Permittivity (nF/m)	$1800 \times \varepsilon_0$
c_{11}^E, c_{22}^E (GPa)	120.3
c_{12}^E (GPa)	75.2
c_{13}^E, c_{23}^E (GPa)	75.1

c_{33}^{E} (GPa)	110.9
c_{66}^{E} (GPa)	22.7
e_{31}, e_{32} (C/m^2)	-5.2
e_{33} (C/m^2)	15.9

The mode sequence and the undamped natural frequencies for the plate-like wing obtained from the FE model close to short-circuit conditions (very low external load resistance) are presented in Table 4. The first five modes are listed where B and T stand for the bending and the torsion modes, respectively. It is important to note that the span-wise elastic axis and the center of gravity are coincident at 50% of chord.

Table 4. Natural frequencies and mode shapes

Mode	Mode shape	ω_{sc} [Hz]
1	1B	1.60
2	2B	10.06
3	1T	16.70
4	3B	27.90
5	2T	50.71

The aeroelastic evolution (damping) for the short-circuit and open-circuit electrical conditions are given in Fig. 3. Five modes are considered in the analysis. The short-circuit and open-circuit flutter speed are similar and determined as 15.8 m/s with the first torsion mode unstable. One can observe a hump mode at 15.8 m/s and the hard crossing occurs at 18.5 m/s. For this particular wing (reduced mass and damping) it is assumed that the flutter speed at the first crossing, the hump mode. A hump mode is a mode that becomes lightly undamped for a limited range of dynamic pressure and then becomes damped again, giving it the characteristic hump shape (Bartels, 2007). Therefore the flutter mode is strongly dominated by torsion motions. For the case investigated here, the flutter speed is not significantly modified since a simple load resistance is used in the electrical domain.

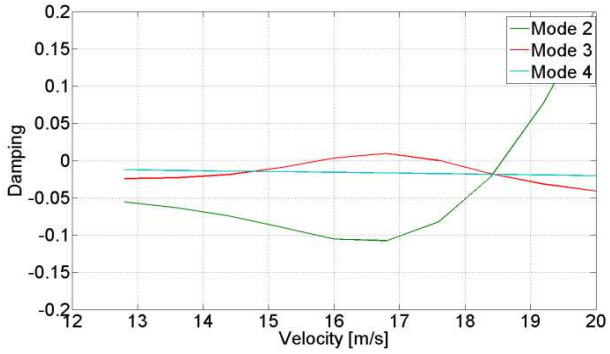

Figure 3. Damping evolution with increasing airflow speed for short-circuit condition.

2.4. Preliminary Experimental Results

This section presents some preliminary experimental verifications for the piezoaeroelastic behavior of a cantilevered plate-like wing with four identical piezoceramics (QP10N, Midé Technology Corporation), two of them on the top and two on the bottom of the plate (Fig. 2). The piezoceramic patches on the same side (A1 and A2) are assumed poled in the same direction and opposed to the pair (B1 and B2) on the other side.

The experimental natural frequencies are obtained from frequency response functions (Figure 4). For this FRF one piezoceramic is used as actuator and other one as a sensor. One can observe for this condition (no flow effect) that the electromechanically coupled FRF successfully predicts the frequencies.

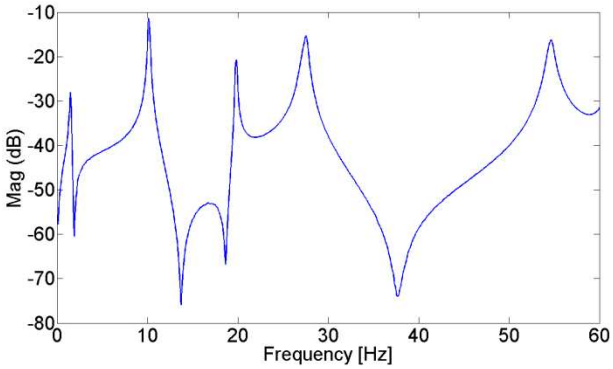

Figure 4. Frequency response function for the uncoupled system

Table 4. Natural frequencies and mode shapes

Mode	Mode shape	ω_{sc} [Hz]	$\omega_{\exp}$ [Hz]
1	1B	1.60	1.50
2	2B	10.06	10.12
3	1T	16.70	19.80
4	3B	27.90	27.54
5	2T	50.71	53.00

The experimental tests were performed in a blower wind tunnel. The open test section dimension is $0.5 \text{ x } 0.5 \text{ m}^2$ and the maximum airflow speed is 20 m/s. The airflow speed is obtained with a simple Pitot tube associated with a micro manometer (TSI-8705). Temperature and atmospheric pressure corrections are also provided. A dSPACE DS 1104 system is used for data acquisition. Four load resistances were tested during the experiments and the flutter boundaries are not significantly modified. At the airflow speed of 18 m/s a typical limit cycle oscillation behavior(Tang and EH Dowell, 2001) is observed. However the linear model cannot predict this nonlinear behavior. It is observed that torsion mode dominates the motions at this airflow speed. The main motivation here is to obtain the voltage output and power output shown in Figs. 5a and b. Voltage output increases with increasing load resistance.

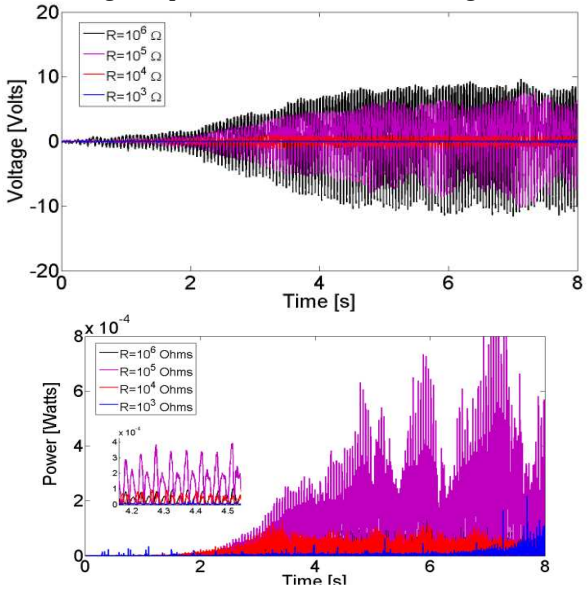

Figure 5. Voltage and power output for different load resistances at the experimental flutter speed (17.5 m/s).

The optimum load resistance among the ones tested here for maximum power output is $R_l = 10^5 \Omega$. The piezoceramics were also connected to avoid the cancellation of electrical output from bending modes. In this case the voltage and power outputs are strongly reduced (as the electrical outputs of the dominant torsional modes are cancelled).

2.5. Conclusion

In this paper, an electromechanically coupled FE plate model based on the classical plate theory is presented for modeling thin piezoelectric generators investigated here. The FE model and an unsteady doublet-lattice method are combined to give the piezoaeroelastic equations, which are solved using a modified pk scheme that accounts the electromechanical coupling. The piezoaeroelastic response of a plate-like generator wing with four piezoceramics is investigated with increasing airflow speed for a set of electrical load resistance. The flutter speed is determined for the short-circuit condition. Since the flutter observed in this work is torsion dominated the piezoceramics are combined to avoid cancelation of the electrical output of torsion modes, The flutter boundaries are not significantly modified when the piezoceramics are combined to avoid cancelation of the electrical output of torsion modes when a set of load resistances are tested in the electrical domain.

Experimental wind tunnel verifications are also presented. The generator wing is tested in a blower wind tunnel. The piezoceramics are also combined to avoid cancelation of the electrical output from torsion modes. Limit cycle oscillation is observed at the airflow speed of 18 m/s. Such behavior cannot be predicted by the linear model presented in this work. The limit cycle behavior is not significantly modified for the set of load resistances considered in this work. However, an optimum load resistance (among the ones tested in this work) is obtained for maximum power output. Further experiments will be conducted for model validations.

3. ACKNOWLEDGEMENTS

The authors also gratefully acknowledge CNPq and FAPEMIG for partially funding the present research work through the INCT-EIE.

4. REFERENCES

Bartels, R.E, Computational aeroelastic modelling of airframes and turbomachinery: progress and challenges*Phil. Trans. R. Soc. A October 15, 2007 365:2469-2499;*

Blair, M. “A Compilation of the mathematics leading to the Doublet Lattice Method”, WL-TR-92-3028,March 1992.

De Marqui, Jr., C., Erturk, A. and Inman, D.J., 2009, “An electromechanical finite element model for piezoelectric energy harvester plates,” Journal of Sound and Vibration, doi: 10.1016/j.jsv.2009.05.015.

De Marqui, Jr., C., Erturk, A., and Inman, D.J. 2009 Effect of Segmented Electrodes on Piezo-Elastic and Piezoaeroelastic Responses of Generator Plates, Proceedings of the ASME Conference on Smart Materials, Adaptive Structures and Intelligent Systems, Oxnard, CA, 20-24 September 2009.

De Marqui, Jr., C., Erturk, A., and Inman, D.J. 2009 Piezoaeroelastically Coupled Modeling and Analysis of Electrical Power Generation and Shunt Damping for a Cantilever Plate, Proceedings of the 17th International Conference on Composite Materials, Edinburgh, UK, 27-31 July 2009.

E. Albano, F. Perkinson and W. P. Rodden, “Subsonic Lifting-Surface Theory Aerodynamics and Flutter Analysis of Interfering Wing/Horizontal-Tail Configurations”,AFFDL-TR-70-59, September 1970.

Erturk, A. and Inman, D.J., 2008, “A distributed parameter electromechanical model for cantilevered piezoelectric energy harvesters,” ASME Journal of Vibration and Acoustics, 130, 041002.

Erturk A. and Inman, D. J. 2009 Issues in Mathematical Modeling of Piezoelectric Energy Harvesters Smart Materials and Structures 17 065016

Erturk, A. and Inman, D.J., 2009, “An experimentally validated bimorph cantilever model for piezoelectric energy harvesting from base excitations,” Smart Materials and Structures, 18, 025009.

J.P. Giesing, T.P. Kalman, W. P. Rodden, “Subsonic Unsteady Aerodynamics for General Configurations, Part I-Vol I-Direct Application of the Nonplanar Doublet Lattice Method”, AFFDL-TR-71-5, November 1971

Rodden, W.P., Jonshon,E.H., “MSC/NASTRAN Aeroelastic Analysis User Guide-Version 68”, The MacNeal-Schwendler Corporation, Los Angeles,CA,1994

Sodano, H.A., Inman, D.J. and Park, G., 2004, “A review of power harvesting from vibration using piezoelectric materials,” The Shock and Vibration Digest, 36, pp. 197-205.

Tang and EH Dowell, Experimental and theoretical study on aeroelastic response of high-aspect-ratio wings, *AIAA Journal* **39** (8) (2001), pp. 1430–1441.

Wang, Q.M. and Cross, L.E., 1999, “Constitutive equations of symmetrical triple layer piezoelectric benders,” IEEE Transactions on Ultrasonics, Ferroelectrics, and Frequency Control, 46, pp. 1343–51.

5. RESPONSIBILITY NOTICE

The authors are the only responsible for the printed material included in this paper.